Optimization of the radar ambiguity function - Application to chaotic sequences

Zouhair Ben Jemaa, Sylvie Marcos, Safya Belghith

Optimization of the Radar Ambiguity Function-Application to Chaotic Sequences

Zouhair Ben Jemaa
Laboratoire RISC
Ecole Nationale d'Ingénieurs de Tunis
Tunis, Tunisia
zouhair.benjemaa@enit.rnu.tn

Sylvie Marcos
Laboratoire L2S, CNRS UMR8506
CentraleSupelec, Université Paris Sud
Paris, France
sylvie.marcos@l2s.centralesupelec.fr

Safya Belghith
Laboratoire RISC
Ecole Nationale d'Ingénieurs de Tunis
Tunis, Tunisia
safya.belghith@enit.utm.tn

***Abstract*—In this paper we propose a statistical approach for the optimization of the phased codes used in radar. By considering each code as a realization of a random variable we show that we can build good codes if the distribution of the random variable is suitably chosen. We then consider sequences generated by the skew tent map and we show that for some values of the bifurcation parameter the invariant probability density coincides with the desired one. To confirm this idea we compute the maximal peak of the ambiguity function outside zero relative to the bifurcation parameter of the skew tent map.**

***Index Terms*—SIMO radar, ambiguity function, chaotic sequences, skew tent map, invariant probability density**

I. Introduction

In radar systems the search for transmitted waveforms leading to the "best possible" ambiguity function, particularly in terms of low side lobes, has already been addressed in the literature [1], [2]. In some works the considered waveforms are defined by a set of sequences; these works aim to design good waveforms by synthesizing sequences having suitable auto- and cross-correlation functions [3], [4], [5], [6], [7]. However, the ambiguity function also depends on parameters concerning the shaping pulse, the geometry of the transmission antenna array and the targets angles of arrival. It also appears that the waveforms generated by the existing methods have drawbacks. Either they are limited in length, or they require important calculations, especially when we need a large number of them or we want to add one.

In the last years chaotic sequences have been considered as an alternative to other sequences in the literature for the design of waveforms in communication systems. Earlier articles in the context of multi-user CDMA communication have already shown the interest of using codes based on chaos over more traditional codes [8], [9]. Some other works have also suggested the use of chaotic sequences as candidates for the design of radar waveforms [10], [11], [12] and the references inside. In this paper we propose a statistical approach in the research of good codes; by considering each code as a realization of a random variable we show that we can build good codes if the distribution of the random variable is suitably chosen. We then consider chaotic sequences generated by the skew tent map and we show that for some values of the bifurcation parameter the invariant probability density coincides with the desired one. To confirm this idea we analyzed the impact of the found results on the ambiguity function; especially on the lobes outside zero relative to the bifurcation parameter of the skew tent map.

After briefly introducing in section II the ambiguity function and extracting the function of interest to be optimized, we will study in section III the statistical properties of the latter. In section IV, we will show how sequences generated by the skew tent map meet the statistical properties established in the previous section and required for a good ambiguity function. Finally the conclusion will summary the contribution of the paper and will present future extensions.

II. Short reminder of the radar ambiguity function

The ambiguity function (AF) of a radar system consists in the 2D output, for a given time delay τ and a given Doppler frequency ν, of the filter matched to the transmitted signal $s(t)$ and can be written as [2]:

$$A(\tau,\nu)=\int s(t)s^*(t+\tau)e^{j2\pi\nu t}dt \tag{1}$$

where the waveform $s(t)$ is given by:

$$s(t)=\sum_{p=1}^{N_c} w_p u(t-(p-1)T_c) \tag{2}$$

where N_c is the length of the sequences $\{w_{m,p}\}_{p=1,N_c}$ and $u(t)$ is a shaping function of duration T_c. (1) then becomes :

$$A(\tau,\nu)=\sum_{p=1}^{N_c}\sum_{l=1}^{N_c} w_p w_l^* \widetilde{\gamma}_{p,l}^u(\tau,\nu) \tag{3}$$

where

$$\widetilde{\gamma}_{p,l}^u(\tau,\nu)=\int u(t-(p-1)T_c)u(t-(l-1)T_c+\tau)e^{j2\pi\nu t}dt \tag{4}$$

For simplicity we will consider in the following the so-called SIMO case where $M=1$ so that $\beta_{m,m'}(\theta,\theta_t)=1$ and the ambiguity function (1) reduces to $A_{1,1}(\tau,\nu)$ that we will note $A(\tau,\nu)$. After some calculations the ambiguity function for $\tau=kT_c$ then becomes:

$$A(kT_c, \nu) = R_w(\nu, k)\alpha(\nu) \tag{5}$$

where

$$\alpha(\nu) = \int_0^{T_c} |u(t)|^2 e^{j2\pi\nu t} dt \tag{6}$$

Note that in the case where $u(t)$ is the rectangular function of support $[0, T_c]$,

$$\alpha(\nu) = e^{j\pi\nu T_c} \frac{\sin \pi\nu T_c}{\pi\nu} \tag{7}$$

In practice, the Doppler frequency ν is usually much smaller than the bandwidth of the probing waveform so that we can safely suppose that $|\frac{\sin \pi\nu T_c}{\pi\nu}| \simeq T_c$. It then appears that the optimization of the ambiguity function reduces to the optimization of

$$|R(k, \nu)| = |\sum_{p=1}^{N_c-k} \omega_p \omega_{p+k}^* e^{j\pi\nu(p-1)T_c}| \tag{8}$$

where $\omega_p = e^{j\pi x_p}$, x_p is a sequence in the interval $[-1, 1]$. The expression (8) becomes

$$|R(k, \nu)| = |\sum_{p=1}^{N_c-k} e^{j\pi z_p(k)}| \tag{9}$$

$$z_p(k) = x_p - x_{p+k} + \nu(p-1)T_c \tag{10}$$

is also a random variable for every fixed integer k.

In the section below we consider the statistics of

$$Z_k = \sum_{p=1}^{N_c-k} e^{j\pi y_p} \tag{11}$$

where y_k is a random variable

III. Statistical properties of $|Z_k|$

A. Statistics of $|Z_k|$ in the case of i.i.d. y_p

Suppose that y_p is i.i.d and the distribution of y_p is symmetrical about its mean zero. From the central limit theorem and for $N_c - k$ large enough the real and imaginary parts of $Z_k = r\exp(j\pi\theta)$ are approximately Gaussian random variable of means $\alpha = E[rcos(\pi\theta)] = (N_c - k)E[cos(\pi y_p)]$ and $\beta = E[rsin(\pi\theta)] = (N_c - k)E[sin(\pi y_p)]$ and variances s_1 and s_2, respectively. The probability distribution of the amplitude $r = |Z_k|$ is, for its part, given by [13]

$$\rho(r) = 2r\sqrt{s_1 + s_2} e^{-(B^2 + (s_1+s_2)r^2)} I_0(2B(s_1 + s_2)r) \tag{12}$$

where $B = \frac{\alpha}{s_1+s_2}$, and I_0 is the modified Bessel function of the first kind.

For example, let us assume that y_p is uniformly distributed in an interval $[-a, a], 0 < a < 1$. It follows that $\alpha = (N_c - k)sinc(a)$ and $\beta = 0$. The distribution (12) of $\rho(r)$ is plotted in Fig. 1 for $a = 1, 0.7, 0.8$. We can see that for a fixed R the probability that $r < R$ is greater for the case $a = 1$ corresponding to the case of uniform distribution of $e^{j\pi y_p}$ on the unit circle. In this case, it is easy to find [13] that $\alpha = 0$ and $s_1 = s_2 = (N_c - k)/2$ so that $B = 0$ and the distribution of $|Z_k|$ reduces to the Rayleigh distribution $\rho(r) = 2\rho\exp(-r^2)$. This latter will be considered as a reference in the sequel (blue line in Fig1). It is easy to show that this case is also obtained if y_p is uniformly distributed on any interval $[k, l]$ where $l - k$ is an even integer.

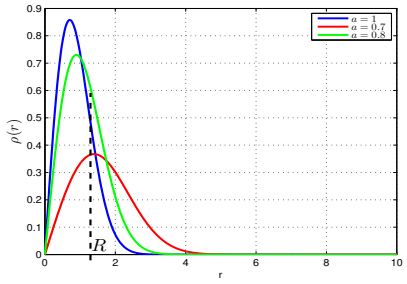

Fig. 1. Distribution of the modulus of $E[Z_k]$

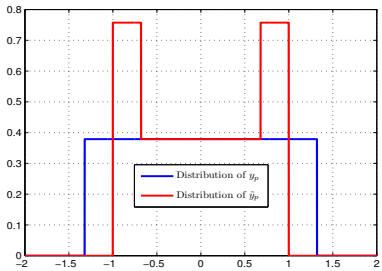

Fig. 2. Distribution of y_p and $\tilde{y}_p$ in the case $1 < a < 2$

More generally, according to [13], whatever the distribution of y_p and whatever R is, the probability $p(r < R)$ will be greater the more the distribution of r will be close to a Rayleigh distribution with $B = 0$.

Now we suppose that y_p is uniformly distributed in an interval $[-a, a]$ where $1 < a < 2$. Because of the periodicity of $e^{j\pi y_p}$ we have $e^{j\pi y_p} = e^{j\pi\tilde{y}_p}$ where $\tilde{y}_p$ is a random variable the distribution of which is shown in Fig.2 in red color. We can see that this distribution is different from the uniform distribution and according to Fig. 4 the histogram of $|Z_k|$ computed over 10000 realizations and for $a = 1.32$ is no longer a Rayleigh distribution and yields high values of the mean and variance of $|Z_k|$.

Let us now assume that y_p has a triangular distribution on the interval $[-2b, 2b], 1 \leq 2b \leq 2$. The distributions of y_p and $\tilde{y}_p$ are plotted together in Fig.3. We can see that $\tilde{y}_p$ is uniformly distributed in $[-1, 1]$ if and only if $b = 1$, i.e. we obtain a uniform equivalent distribution in the interval $[-1, 1]$ if the distribution of y_p is a triangle on the interval $[-2, 2]$. We can see on Fig. 4 the influence of the definition interval $[-2b, 2b]$ of the triangle distribution on the histogram of $|Z_k|$. If $b = 1$, the distribution of $|Z_k|$ is of Rayleigh type with minimal mean and

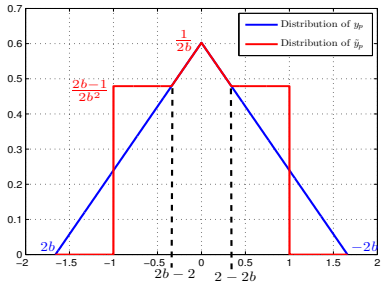

Fig. 3. Distribution of y_p and $\tilde{y}_p$ in the case of triangular distribution

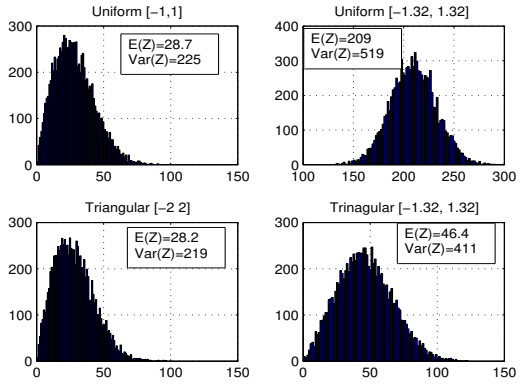

Fig. 4. Histograms of $|Z_k|$ in the case of uniform and triangular distributions

variance whereas for $2b = 1.32$ it is no longer of a Rayleigh type and yields a high mean and variance. Also note that it is easy to compute $\alpha = (N_c - k)[1 - \cos(\pi 2b)]/4b^2\pi^2$ which is zero for $b = 1$ (and consequently $B = 0$).

B. Statistics of Z_k in the case $y_p = x_{p+k} - x_p$

For a fixed integer k let $y_p = x_{p+k} - x_p$. If the x_p are i.i.d random variables uniformly distributed in the interval $[-a, a], 0 < a < 1$ the distribution of y_p is the triangular function on the interval $[-2a, 2a]$. If $2a < 1$ the distribution of y_p is triangular within the interval $[-1, 1]$ and thus differs enough from the uniform distribution to give bad mean and variance of $|Z_k|$ as explained in the previous section. If $2a > 1$ we retrieve the statistics of $|Z_k|$ described in the previous section, i.e. optimum is $2a = 2$. More generally, the distribution of the x_p may not be a uniform one, the key is to have y_p with a triangular distribution on the interval $[-b, b]$ with $b \geq 2$. We will see in section IV a way of generating such x_p.

C. Statistics of Z_k in the case $y_p = u_p + \nu(p-1)T_c$

We here consider the statistics of

$$y_p = u_p + \nu(p-1)T_c \tag{13}$$

where u_p are i.i.d. random variables. The presence of the deterministic term $\nu(p-1)T_c$ in the expression of y_p makes difficult to analyze the statistics of $|Z_k|$. However, it is easy

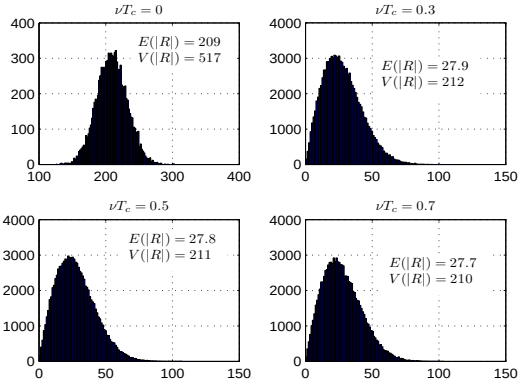

Fig. 5. Histograms of $|Z_k|$ in the case of y_p uniform in $[-1.2, 1.2]$

to see that as the u_p are i.i.d. $E[e^{j\pi u_p}]$ is a constant denoted by A and

$$E[Z_k(\nu)] = A \sum_{p=1}^{N_c-k} e^{j\pi(p-1)\nu T_c} \tag{14}$$

In case $\nu T_c = 2q$ where q is an integer, $E[Z_k(\nu)] = A(N_c - k)$. If $A = 0$ the real part of $Z_k(\nu)$ is also zero and consequently $\alpha = 0$ and $B = 0$ which are the conditions so that $|Z_k|$ has a Rayleigh type distribution (see [13]).
In case $\nu T_c \neq 2q$:

$$E[Z_k(\nu)] = A \frac{e^{j\pi(N_c-k)\nu T_c}/2}{e^{j\pi\nu T_c/2}} \frac{\sin[\pi(N_c-k)\nu T_c/2]}{\sin[\pi\nu T_c/2]} \tag{15}$$

Since $|\sin[\pi(N_c-k)\nu T_c/2]| \leq (N_c-k)|\sin[\pi\nu T_c/2]|$, we obtain

$$Real(E[Z_k(\nu)]) \leq |A|(Nc-k) \tag{16}$$

Also in this case if $A = 0$, the real part of $E[Z_k(\nu)]$ is zero, thus $\alpha = 0$ and $B = 0$ which are the conditions so that $|Z_k|$ has a Rayleigh type distribution. To illustrate this idea we plotted in the Fig.5 the histograms of $|Z_k|$ for y_p uniformly distributed in $|-1.2, 1.2]$; we can see that the distribution of $|Z_k|$ differs from the desired Rayleigh one only when $\nu = 0$. This could be explained by saying that the presence of the deterministic term in (13) allows uniform scattering of the points on the unit circle when the distribution of u_p is not uniformly distribution in $[-1, 1]$.

D. Summary

We can summarize the following points

- If we aim to minimize $|Z_k| = |\sum_{p=1}^{k} e^{j\pi y_p}|$ by assuming $y_p, p = 1, 2, ...k$ are k realizations of a uniform random variable in $[-a, a]$, the optimum is obtained for $a = 1$, i.e. y_p uniformly distributed in the interval $[-1, 1]$.
- Due to the periodicity of $e^{j\pi y_p}$ this optimum can also be achieved by other distributions of y_p, this has been examplified with a triangular distribution on the interval $[-2, 2]$.

- If $y_p = x_{p+k} - x_p$, the above condition can be obtained if x_p is uniformly distributed in the interval $[-1, 1]$.
- Looking for sequences that minimizes $|Z_k| = |\sum_{p=1}^{k} e^{j\pi(x_{p+k}-x_p+\nu(p-1)T_c)y_p}|$ reduces to cancelling the term for $\nu = 0$.

IV. Sequences generated by the skew tent map

In this section we consider chaotic sequences x_p generated by $x_{p+1} = T_\mu(x_p)$ and an initial condition x_0 where $T_\mu(x)$ is the piece-wise linear skew tent map defined in $[-1, 1]$ by

$$T_\mu(x) = \begin{cases} \frac{2}{\mu-1}x - \frac{1+\mu}{\mu-1} & if \quad \mu < x \leq 1 \\ \frac{2}{\mu+1}x - \frac{\mu-1}{\mu+1} & otherwise \end{cases} \tag{17}$$

The invariant probability density of the variable x_p is the uniform distribution in the interval $[-1, 1]$ [14] i.e. x_p could be considered as a realization of a uniform random variable uniformly distributed in $[-1, 1]$. The idea is to use such sequences in the MIMO radar system described above with $y_p = T_\mu^k(x_p) - x_p$.
The map $y = T_\mu^k(x) - x$ is plotted in Fig.6. The minimum and

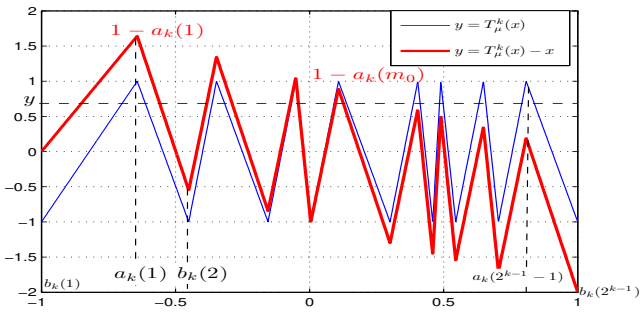

Fig. 6. Curves of $y = T_\mu^k(x) - x$

the maximum are respectively $(a_k(m), 1 - a_k(m)), 1 \leq m \leq 2^{k-1}$ and $(b_k(m), -1 - b_k(m)), 1 \leq m \leq 2^{k-1}+1$; $a_k(m)$ and $b_k(m)$ are defined by the following recursive relations [15]:

$$a_1(1) = \mu, \quad b_1(1) = -1, \quad b_1(2) = 1$$

$$a_{k+1}(2m-1) = \frac{\mu+1}{2}[a_k(m) - b_k(m)] + b_k(m)$$

$$a_{k+1}(2m) = \frac{\mu+1}{2}[a_k(m) - b_k(m+1)] + b_k(m+1)$$

$$b_{k+1}(2m-1) = b_k(m)$$

$$b_{k+1}(2m) = a_k(m)$$

$$b_{k+1}(2m+1) = b_k(m+1)$$

Let

$$\begin{aligned} A(k,m) &= \tfrac{a_k(m)-b_k(m)}{2-a_k(m)+b_k(m)} \\ C(k,m) &= \tfrac{a_k(m)-b_k(m+1)}{2-a_k(m)+b_k(m+1)} \end{aligned} \tag{18}$$

and $M = 1 - a_k(1)$ and $m = -1 - b_k(2^{k-1}+1)$; we show that if x follows the uniform distribution in the interval $[-1, 1]$ then the probability density $f_{\mu,k}(y)$ of $T_\mu^k(x) - x$ is zero outside $[m, M]$ and for every $y \in [m, M]$ $f_{\mu,k}(y)$ is

$$f_{\mu,k}(y) = \frac{\sum_{m=1}^{m_0}[A(k,m) - C(k,m)]}{2} \tag{19}$$

where m_0 is such that $y \in [1 - a_k(m_0+1), 1 - a_k(m_0)]$. Fig. 7 and 5 exhibit the probability density of $y = T_\mu^k(x) - x$ in blue line for $\mu = 0.1$ and $\mu = 0.7$ and for different values of k. In red line we plotted the probability density of the equivalent $\hat{y}$ of y; from the previous discussion $\hat{y}$ should be uniform in the interval $[-1, 1]$. We can see that after a few

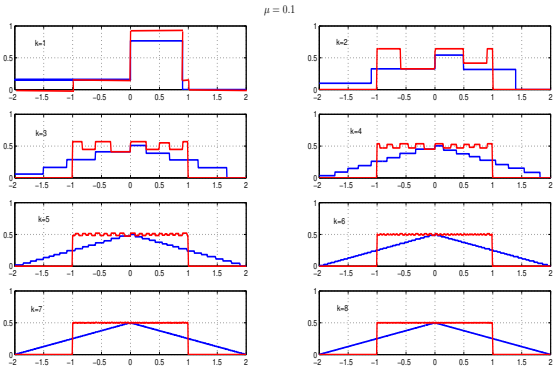

Fig. 7. Probability density of $T_\mu^k(x) - x$ for $\mu = 0.1$

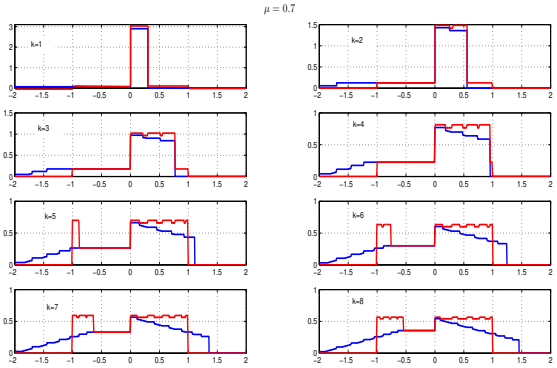

Fig. 8. Probability density of $T_\mu^k(x) - x$ for $\mu = 0.7$

iterations the probability density of $y = T_\mu^k(x) - x$ tends to the triangular distribution in the interval $[-2, 2]$ and thus $\hat{y}$ follows the uniform distribution in the interval $[-1, 1]$ for all values of μ, subsequently we have to look for parameter μ that allows good probability densities for the first iterations.

To measure the resemblance of $f_{\mu,k}(y)$ with the uniform distribution on the interval $[-1, 1]$ we considered the criteria

$$C(\mu, k) = \int_{-1}^{1} (f_\mu(x) - \frac{1}{2})^2 dx \tag{20}$$

We plotted in Fig.9 the criteria $C(k, \mu)$ versus the iteration number k and for different values μ. It is clear that the case

$\mu = 0.1$ allows the best value of $C(k, \mu)$.

To see the impact of this result on the performance of the

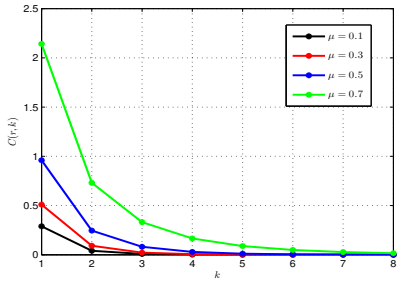

Fig. 9. $C(\mu, k)$ for different values of μ and k

radar system we plotted in Figures 10 to 12 the function (9) for $\mu = 0.1$ and $\mu = 0.7$ and for the first values of k, i.e. $k = 1, 2, 3$. As expected via the above analysis, the case $\mu = 0.1$ allows low peaks in (9) yielding a better ambiguity function.

In Fig.13 and 14 we plotted the ambiguity function (10)

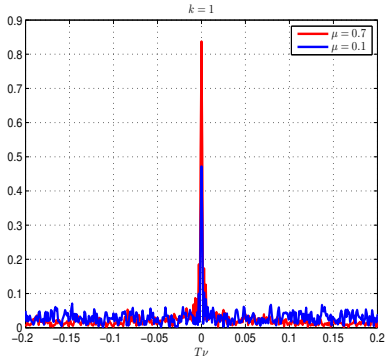

Fig. 10. $|R(1, \nu)|$ for $\mu = 0.1$ and $\mu = 0.7$

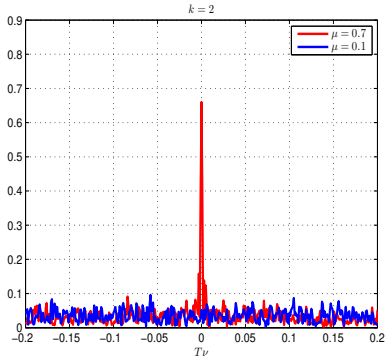

Fig. 11. $|R(2, \nu)|$ for $\mu = 0.1$ and $\mu = 0.7$

when the codes x_k are generated by the skewtent map (18) for $\mu = 0.1$ and $\mu = 0.7$. We can see the difference between

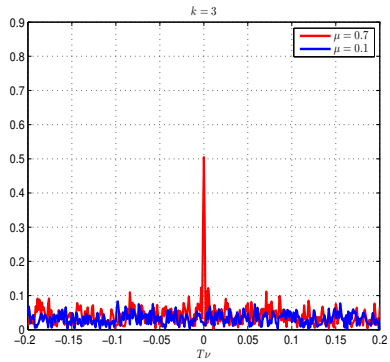

Fig. 12. $|R(3, \nu)|$ for $\mu = 0.1$ and $\mu = 0.7$

the two functions, especially for $\nu \cong 0$, $\nu \cong 2$ and $\nu \cong -2$; indeed around these values the peaks are higher for $\mu = 0.7$ which confirms the found results.

In Fig.15 we plotted the maximal peak of the ambiguity func-

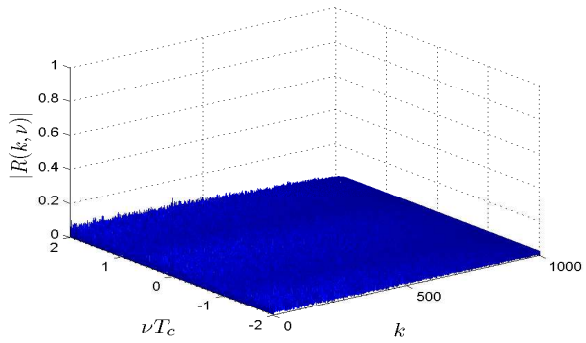

Fig. 13. $|R(k, \nu)|$ for $\mu = 0.1$

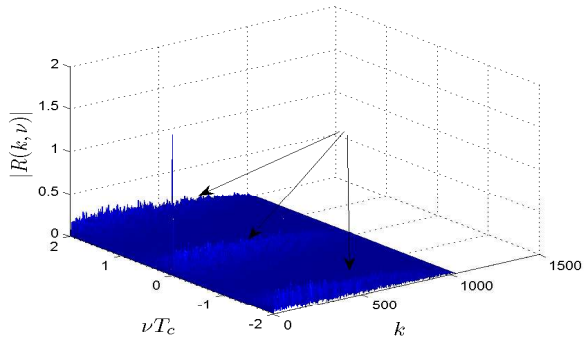

Fig. 14. $|R(k, \nu)|$ for $\mu = 0.7$

tion and the Lyapunov exponent (the well known parameter which characterizes the unstability of a dynamical system) versus the bifurcation parameter μ. We can see that the more chaotic the sequences, the better the ambiguity function.

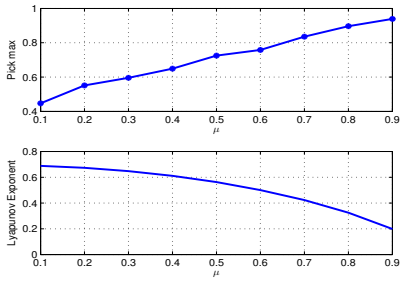

Fig. 15. Maximal peak of the ambiguity function and Lyapunov exponent versus the bifurcation parameter μ

V. Conclusion

In this paper we adopted a statistical approach to look for sequences allowing optimization of the ambiguity function of a radar system. We have shown that good sequences can be generated by a random variable with a suitable distribution and that it is possible to obtain such sequences by generating them using a chaotic skew tent map. Because of the promising results we have obtained, we will examine the MIMO case in future work and adopt the same statistical approach to optimize the ambiguity function by considering the inter-correlation functions of the sequences.

References

[1] J. J. Benedetto, I. Konstantinidis ; M. Rangaswamy , "Phase-Coded Waveforms and Their Design," IEEE Signal Processing Magazine, vol. 26, N° 1, pp 22-31, Janv 2009.

[2] J. Li and P. Stoica, MIMO radar signal processing. John Wiley and Sons Inc., New Jersey, 2009.

[3] H. Sun, F. Brigui and M. Lesturgie, "Analysis and comparison of MIMO radar waveforms," 2014 International Radar Conference, Lille, France, August 13-17 october 2014.

[4] P. Stoica, H. He and J. Li, "On designing sequences with impulse-like periodic correlation," IEEE Signal Processing Letters, vol. 16, N°8 pp. 703–706, August 2009.

[5] H. He, P. Stoica and J. Li, "Designing unimodular sequence sets with good correlations - including an application to MIMO radar," IEEE Trans. on signal processing, vol. 57, N°11 pp. 4391–4405, November 2009.

[6] F. Arlery, R. Kassab, U. Tan and F. Lehmann, "Efficient gradient method for locally optimizing the periodic/aperiodic ambiguity function", Proceedings of IEEE Radar Conference (RadarConf), Philadelphia, PA, USA, 2016.

[7] U. Tan, C. Adnet, O. Rabaste, F. Arlery, J-P. Ovarlez and J-P. Guyvarch, "Phase code optimization for coherent MIMO radar via a gradient descent," 2016 IEEE Radar Conference (RadarConf), Philadelphia, PA, United States, May 2016.

[8] Mourad Khanfouci and Sylvie Marcos. "PLM sequences for the performance optimization of linear multiuser detectors," Proceedings of EUSIPCO 2005, Sept 2005, Antalya, Turkey.

[9] Soumaya Meherzi, Sylvie Marcos and Safya Belghith. "A family of spatiotemporal chaotic sequences outperforming Gold ones in asynchronous DS-CDMA systems," Proceedings of EUSIPCO 2006, Sept 2006, Florence, Italy.

[10] Z. Ben Jemaa and S. Belghith, "Chaotic sequences with good correlation properties for MIMO Radar application," 2016 IEEE SoftCom Conference (RadarConf), Split, Croatia, September 2016.

[11] M.S. Willsey, "Quasi-orthogonal wideband radar waveforms based on chaotic systems". Master of engineering thesis, Massachussets Institute of Technology (MIT), Cambridge, MA, United states, 2006.

[12] Y. Jin, H. Wang, W. Jiang and Z. Zhuang, "Complementary-based chaotic phase-coded waveforms design for MIMO radar," IET Radar, Sonar and Navigation, vol. 7, N°4 pp. 371–382, 2013.

[13] P. Beckmann, "Statistical Distribution of the Amplitude and the Phase of a Multiply Scattered Field," Journal of Research of the National Buureau of Standards-Radio Propagation, vol. 66D, No. 3, pp. 231–240, Mai-Juin 1962.

[14] M. Eisencraft, D.M.Kato, L.H.A.Monteiro, "Spectral properties of chaotic signals generated by the skew tent map," Signal Processing 90, pp. 385-390 (2010).

[15] Z. Ben Jemaa , D. Fournier-Prunaret , S. Belghith, "Kendall's tau based correlation analysis of Chaotic Sequences generated by piecewise linear maps," International Journal of Bifurcation and Chaos Vol. 25, No. 13, 1550177 (2015).